12^{th} International Conference on Fracture Mechanics of Concrete and Concrete Structures
FraMCoS-12
B.L.A. Pichler, Ch. Hellmich, P. Preinstorfer (Eds)

https://doi.org/10.21012/FC12.1208
MS13-2:4

DAMAGE EVOLUTION AND FRACTURE BEHAVIOUR OF UNDER-REINFORCED CONCRETE BEAMS USING ACOUSTIC EMISSION TECHNIQUE

PRASHANTH M. H * **and J. M. CHANDRA KISHEN**‡

* Associate Professor
National Institute of Technology Karnataka
Surathkal, Mangalore, India
e-mail: mhprashanth1@gmail.com

‡Professor
Indian Institute of Science, Bangalore, India
e-mail: chandrak@iisc.ac.in

Key words: Fracture, under-reinforced concrete beam, reinforcement, acoustic emission

Abstract. In this study, an experimental work was carried to focus on damage evolution and fracture behavior of under-reinforced concrete beams by continuously monitoring using acoustic emission technique. Beams were of three different sizes with geometric similarity having single longitudinal reinforcement without stirrups. The specimens was tested in three point loading under CMOD control in the closed loop servo controlled hydraulic testing machine. The results of load, displacement, CMOD and strain in the steel are acquired in the data acquisition system. The results of acoustic emission such as location, hits, events, amplitude, absolute energy and time were also simultaneously stored in a computer during the testing.

The results of acoustic emission such as spread of the events and its distribution within the beams help in understanding the fracture processes. They provide information regarding the sequence of mechanisms taking place such as micro-cracking, coalescing of microcracks to macrocracks, increased width of macro-cracking and final fracture in under-reinforced concrete beams.

.

1 Introduction

The behaviour of reinforced concrete depends on the combined action of the concrete and its embedded reinforcement. This composite action is produced by the bond stress at the interface of the two materials. The study of reinforced concrete is complex due to microstructural changes in concrete alone and interaction between the steel and concrete and the bond between them. There may be other failure mechanisms involved in reinforced concrete such as yielding and slippage of steel and delamination between steel and concrete. The reinforcement provided in beams should be such that they prevent unstable crack propagation and avoid brittle failure due to concrete crushing. Reinforced concrete (RC) structures are commonly designed to satisfy two criteria: serviceability and safety. In addition, they are required to show ductile response under the action of various combinations of loadings. To ensure the serviceability requirement, it is necessary to correctly predict the cracking and deflections of reinforced concrete structures under working loads. To assess the safety of structures against collapse, an accurate estimation of the ultimate load is essential and ductility is necessary in order to give ample warning of the incipient collapse by the development of large deformations prior to collapse.

Very few researchers have attempted to study the damage evolution and fracture behavior of lightly and under-reinforced concrete beams. Ruiz et al. [1] experimentally studied the fracture of lightly reinforced concrete beams and examined the sensitivity to size and the bonding properties of steel to concrete.They concluded that lightly reinforced beams show size effect in relation to the maximum load and their ultimate strength is directly proportional to the steel ratio. Sumarac et al. [2] studied the fracturing of reinforced concrete beams subjected to three point bending analytically (using the principles of fracture mechanics), computationally and experimentally. They found that, the optical and graphite sensors were successfull in estimating the location of the crack front. Fantilli et al. [3] investigated experimentally the effect of bar diameter on the behavior of lightly reinforced concrete beams and concluded that the bending moments that characterize the softening branch at the formation of the first crack is significantly dependent on the bar diameter. Ruiz and Carmona [4] examined experimentally the effect of shape of cross section and arrangement of rebar on the fracturing of lightly reinforced concrete beams. They concluded that lightly reinforced beams exhibit a shape effect at the maximum load, similar to the size effect. Momoki et al. [5] used the acoustic emission technique to assess the behaviour of plain concrete beams under flexural loading and a composite made of vinyl fibre-reinforced mortar layer. Their study showed that parameters of AE could be used to differentiate between the modes of flexure and shear fracture that occurred during the loading. Kaphle et al. [6] explored various tools for analysing AE data from structural health monitoring of civil, mechanical, and aerospace structures. They have dealt with two primary challenges, i.e. differentiating signals from different sources and quantifying amounts of damage for severity assessment. Carpinteri et al. [7] used the acoustic emission technique to perform damage analysis on reinforced concrete buildings. The AE activity was correlated with the size of the source crack advancements through fitting relationships, using models from theories of damage mechanics, fracture mechanics and geophysics. Vidya Sagar and Rao [8] studied damage characterization of reinforced concrete beams using AE based b-value analysis. They monitored the fracture process in RC beams subjected to cyclic loading and observed that b-value analysis is useful in assessing the damage level in RC structures in site. Vidya Sagar [9] studied about acoustic emission characteristics of reinforced concrete beams with varying percentage of tension steel reinforcement under flexural loading. Reinforced concrete (RC) flanged beam specimens were tested under incremental cyclic load till failure in flexure. He proposed a relation between the total AE energy released and percentage of steel in RC beams. It was also observed that, as the percentage of steel present in the test specimen is increased, the loading cycle number entering into the heavy damage zone in NDIS-2421 damage assessment chart also increased. Carni et al. [10] studied the damage analysis of concrete structures by means of acoustic emissions (AE) signal analysis. The analysis of the AE signal is based on the Gutenberg Richter law (GBR), which expresses the relationship between magnitude and total number of earthquake events in a defined region and time interval. On the basis of the GBR law, the AE signals identifying critical damage are selected and the proposed procedure is validated experimentally through compression tests carried out on cubic concrete specimens. Lacidogna et al. [11] monitored the damage of three point bending concrete specimens by acoustic emission and natural frequency analysis. Average frequency vs. RA value analysis was used to characterize the crack propagation mode, whereas the cumulative AE energy and the variation in the resonant bending frequencies were selected as the main parameters to monitor the damage progress due to crack advancement. An inverse procedure was applied to estimate the crack advancement based on the measured and calculated frequencies. Prashanth et al. [12, 13] studied the role of steel reinforcement in under reinforced concrete beams when subjected to flexural fatigue loading using the acoustic emission (AE) technique. In this work, three-point bend notched beams of three different sizes and with varying reinforcement ratios were subjected to stepwise increasing variable amplitude fatigue loading. It was concluded that the acoustic emission technique was useful in monitoring and understanding the behavior and crack growth of the under reinforced beam specimens and the presence of reinforcement substantially increased the fatigue life. Apart from the few attempts by the researchers to study the fracture behavior of lightly and under-reinforced concrete beams, very little information has been reported in the literature on the use of AE technique for monitoring and assessing the damage evolution and behavior of under-reinforced concrete beams.

The main objective of the work presented in this paper is to study the damage evolution and fracture behavior of under-reinforced concrete beams of three different sizes having single longitudinal reinforcement. The acoustic emission technique is used for monitoring the behavior and crack growth of the under reinforced specimen. The results of acoustic emission location, hits, events, amplitude, absolute energy and time are used to analyze the damage evolution, fracture behavior and failure mechanisms.

2 Experimental program

2.1 Materials and mix proportions

Ordinary Portland cement (OPC) 53 grade of specific gravity 3.15 was used in casting of concrete specimens. The Locally available natural sand was used as fine aggregate. The specific gravity of fine aggregate was 2.7 and fineness modulus was 2.2. The locally available crushed granite metal with specific gravity of 2.8 was used as coarse aggregate and maximum size of 12.5 mm was used. The concrete mix of grade $M40$ was arrived according to ACI method. The mix proportion of cement, fine aggregate, coarse aggregate and water was 1:1.86:2.60:0.54 by weight. The companion concrete had the compressive strength of 51 MPa, modulus of elasticity of 35,400 MPa and split tensile strength of 3.55 MPa. The reinforcement used were high yield strength deformed steel bars of grade Fe500 whose tested yield stress was 520 MPa, tested Modulus of Elasticity was 20200 MPa, and measured elongation at break was 10%. An electrical resistance strain gauge of 120 ohms is mounted on mid-length of steel bar prior to casting of beam specimens.

The geometrically similar specimens were of length to depth ratio (L/d) of 4.5, span to depth ratio (S/d) of 4, and notch to depth ratio (a_0/d) of 0.2. The thickness (B) is 50 mm which is constant for all sizes of specimens. The beam specimens were reinforced with single longitudinal bar and no shear reinforcement (stirrups) were provided. In the present experimental work, the design of under-reinforced sections for small and medium size were obtained using a single reinforcing bar of diameter 6mm and for large sized specimens using a single reinforcing bar diameter of 6mm and 8mm. The reinforcement is provided 12mm above the initial notch tip. The geometric details of specimens are shown in Figure 1. The details of dimensions of small, medium and large specimens with reinforcements are shown in Table 1 and Figure 2.

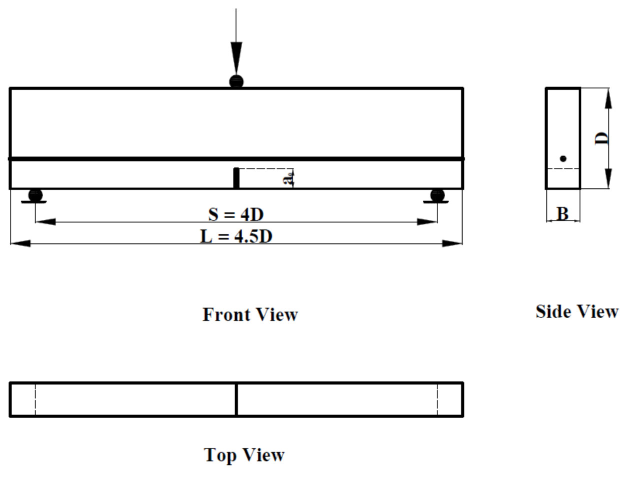

Figure 1: Details of geometry of the specimens

Table 1: Details of dimensions of beam

Beam Size	D (mm)	S (mm)	L (mm)	a_0	ϕ	p_t (%)
S	75	300	337.5	15	6	0.75
M	150	600	675	30	6	0.37
L	300	1200	1350	60	6	0.18
L	300	1200	1350	60	8	0.33

Dimension - **D** -Depth, **S** - Span, **L** - Length
Beam Size - **S** - Small, **M** - Medium, **L** - Large
a_0 is Notch size in mm.
ϕ-Bar diameter in mm.
$p_t(\%)=(A_{st}/BD)*100$

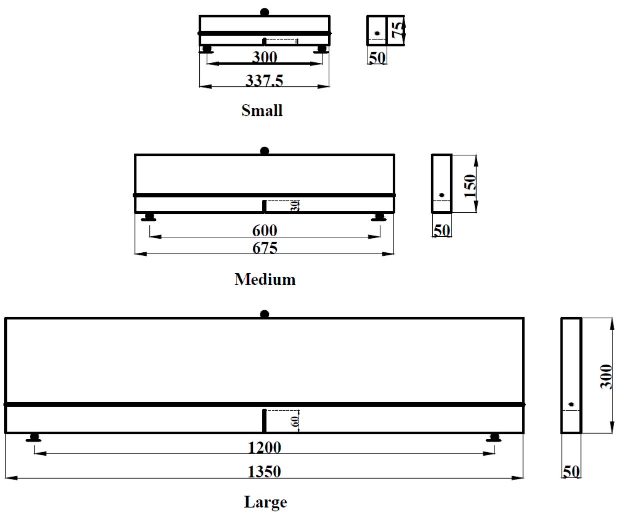

Figure 2: Geometrically similar specimens

2.2 Testing of specimens

The specimens were tested on high stiffness testing machine of load capacity 35 kN with servo controlled hydraulic actuator system having closed loop control. The testing of beam specimen and instrumentation used are shown in Figure 3. An in-built load cell of 35 kN was used for measuring the load. The load point displacement was measured using linear variable displacement transformer (LVDT). The crack mouth opening displacement (CMOD) was measured using the clip gauge. All the tests were performed in CMOD control at the rate of opening of 0.001 mm/sec. The results of load, CMOD, displacement and time are simultaneously acquired through a data acquisition system. In order to obtain the 3D location of AE-events, six AE-sensors are mounted on the specimen for medium and large specimen as shown in Figure 4 with three sensors in the front and three on the back face. Four sensors are mounted on the small specimen as shown in the Figure 4 with two sensors in front and two on back face. The AE data such as hits, events, energy, absolute energy, signal strength, spatial positions, amplitude and time are simultaneously acquired using a seperate data acquisition system during the experiments. The AE sensors used in the experimental work are resonant type differential sensors R6D. The diameter and height of AE sensors are 19 mm and 22 mm, respectively. These sensors can function at an operating frequency of 35 to 100 kHz. For sensor, couplant used was high vacuum silicon grease. The AE signals were amplified with a gain of 40 dB using a pre-amplifier. An eight-channel AE-WIN for SAMOS E2.0 (Sensor based Acoustic Multichannel Operating System), developed by Physical Acoustics Corporation (PAC)-USA has been used for AE data acquisition. A threshold of 40 dB was adopted in AE testing for concrete.

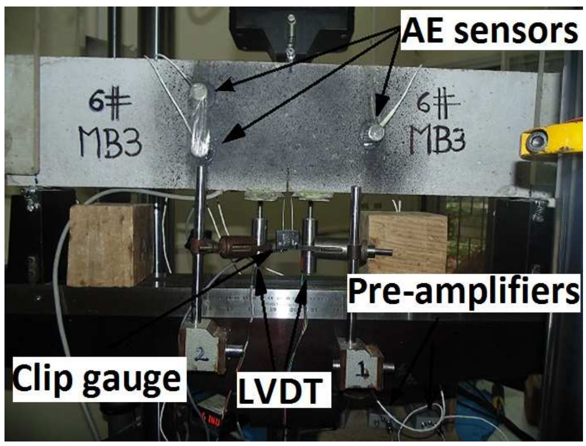

Figure 3: Testing of beam specimen and instrumentation such as clip gauge, LVDT, AE sensors and preamplifiers

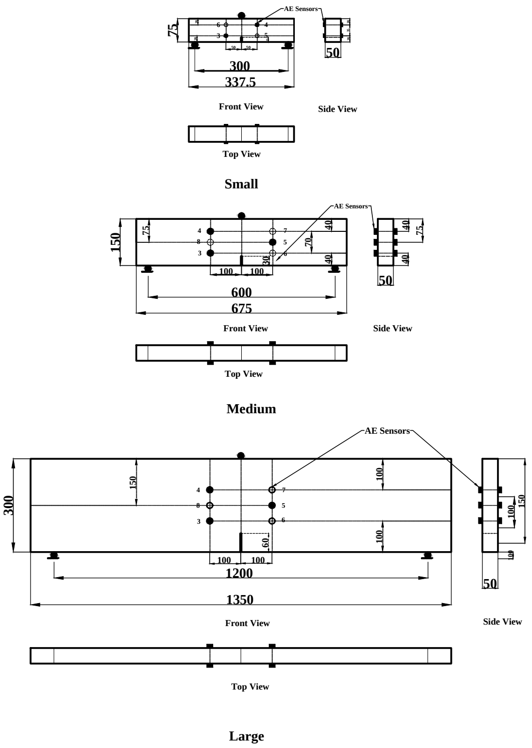

Figure 4: AE sensor location for the small, medium and large size specimens

3 Results and discussions from mechanical testing

The experimental data such as load, CMOD, mid-span displacement and strain, acquired during the tests are analysed. The present experimental work aims to understand the fracture behavior of a under-reinforced concrete beams of different sizes with single longitudinal reinforcement.

The medium size specimen with 6mm diameter bar (0.37%) is chosen to explain the typical fracture behavior of under-reinforced concrete beam shown in Figures 5 6 7 . The plot of load versus mid-span displacement in Figure 5 shows salient points A, B, C, D, E, F to understand the behaviour. Load versus displacement relation is linear until the point A and entire load is taken by concrete. At point A, micro cracks begin to form at the bottom of the midspan and these micro cracks propagate to the level of reinforcement upto around the point B. Point B corresponds to the first peak beyond which there is a drop in the load carrying capacity upto point C. Around the point C, a band of intensive micro-cracking and damage takes place at the midspan section. This is the reason for the drop in load between points B and C. At point C, the load increases with increasing strain in steel as seen in the plot of Figure 7 at which stage the load has started to transfer from concrete to steel and the micro cracking has started to propagate beyond the level of reinforcement. The cracking propagates in the direction, approaching the point of loading, till the point D. From the points D to E, continuous yielding and elongation of reinforcement bar is taking place with the subsequent formation of plastic zone in the steel bar with increasing ductility of the beam specimen. From point E to F, the elongation of reinforcement bar is leading to a reduction in its cross section with gradual reduction in the load carrying capacity of beam specimen finally leading to failure. Strain readings in the steel beyond point D could not be obtained because of the failure of the strain gauge during plastic yielding.

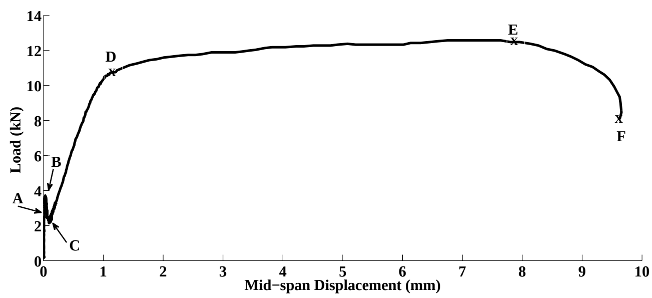

Figure 5: Salient points in plot of Load versus Mid-span Displacement for typical medium size specimen with 6mm diameter (0.37%)

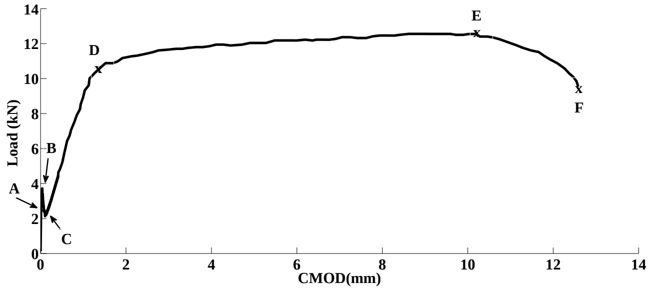

Figure 6: Salient points in plot of Load versus CMOD for typical medium size specimen with 6mm diameter (0.37%)

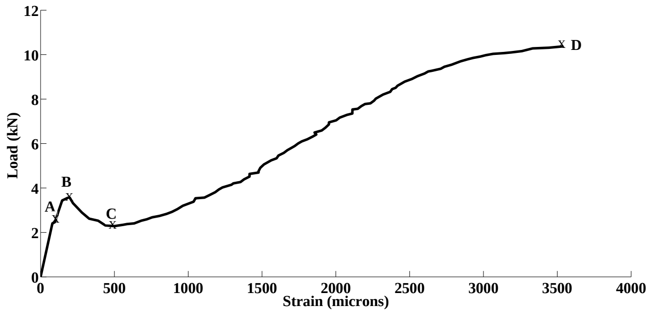

Figure 7: Salient points in plot of Load versus Strain for typical medium size specimen with 6mm diameter (0.37%)

Figure 8 Figure 9 and Figure 10 shows the results of load versus CMOD, load versus displacement at midpoint and load versus strain in rebar respectively for small, medium and two large beams.

From the load versus CMOD and load versus midspan displacement plots of Figures 8 9, it is seen that the slopes of initial segment are overlapping with each other for all sizes and reinforcement ratios of beams. This is due to the fact that only the stiffness of plain concrete is reflected and the reinforcement has not yet come into action. The first peak in the load corresponds to the capacity of plain concrete which has started to crack. There is a drop in the load carrying capacity with increasing displacements until the crack reaches the reinforcement after which the load transfer mechanism shifts to the steel bar. Figure 10 shows that there is a substantial increase of longitudinal strain in the rebar beyond the first peak load. The maximum load is reached in the respective beams when the strain in the rebar has reached its yield value which is in the range of 3500 to 3800 microstrains. As the plastic strains increase in the reinforcement the CMOD and mid-span displacement increases substantially at constant load indicating a ductile behavior which is the main characteristic of under-reinforced concrete beams. The salient characteristics of all the beams with their numerical values are given in Table 2.

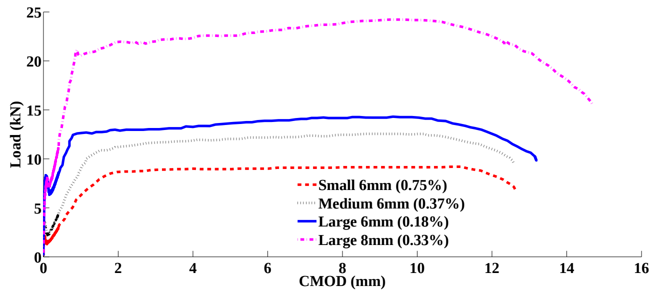

Figure 8: Load versus CMOD for small 6mm (0.75%), medium 6mm (0.37%), large 6mm (0.18%) and large 8mm (0.33%) specimens

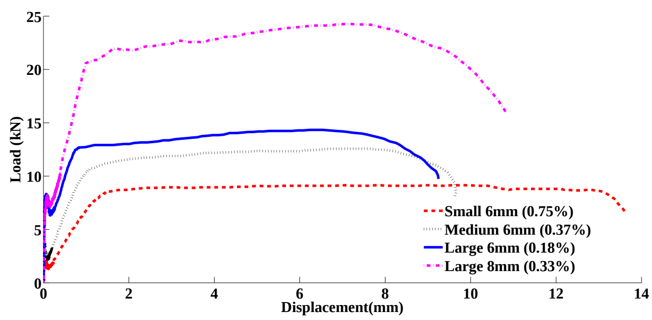

Figure 9: Load versus Displacement for small 6mm (0.75%), medium 6mm (0.37%), large 6mm (0.18%) and large 8mm (0.33%) specimens

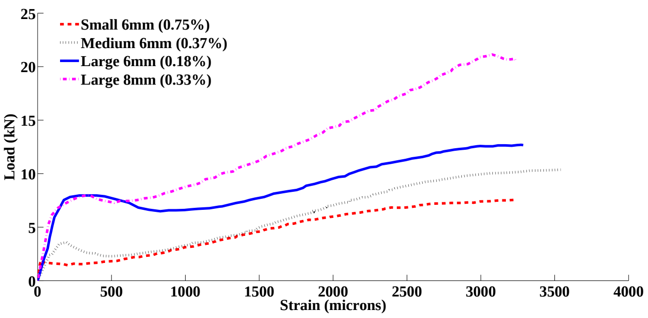

Figure 10: Load versus Strain in rebar for small 6mm (0.75%), medium 6mm (0.37%), large 6mm (0.18%) and large 8mm (0.33%) specimens

Table 2: Details of testing results

Beam size Bar dia p_t(%)	Small 6mm 0.75%	Medium 6mm 0.37%	Large 6mm 0.18%	Large 8mm 0.33%
Cracking load(kN)	1.95	3.62	8.28	8.20
Load at yielding(kN)	8.54	10.57	12.52	20.99
Ultimate load(kN)	9.10	12.57	14.33	24.22
Displacemt at cracking(mm)	0.04	0.03	0.07	0.09
Displacemt at yielding(mm)	1.45	1.08	0.75	1.08
Displacemt at failure(mm)	13.63	9.63	9.25	10.85
CMOD at cracking(mm)	0.04	0.035	0.06	0.11
CMOD at yielding(mm)	1.80	1.33	0.90	1.11
CMOD at failure(mm)	12.62	12.58	13.19	14.64
Ductility	9.39	8.91	10.05	12.28
Initial stiffness (kN/mm)	201	212	222	230
Mechanical energy (kNmm)	115	110	121	235

4 Results and discussions on acoustic emission

4.1 AE events and absolute energy

AE events are a result of micro cracking in the concrete material and spread of these events indicate micro crack distribution and the spread of damage [14]. The medium size specimen with 6mm diameter bar (0.37 %) is typically chosen to explain the fracture behavior of under-reinforced concrete beam through acoustic emission. Picture in Figure 11 shows the front and side views of AE events at different points of loading until yielding with corresponding numbers for the medium size specimen with 6mm diameter bar (0.37%) shown in load and cumulative events versus time plot of Figure 12. Picture in Figure 13 shows the AE events for further points of loading as shown in Figure 14 of the complete cumulative events and load with time until fracture.

Based on the discussions in the previous section and the observations in Figure 12, the beam behaves elastically until point 1 on the load-time curve wherein the cracking gets initiated from the notch. The behavior of the beam is linear until about 80% of the first peak load (point 1) after which microcracking begins. Until point 1, the acoustic emission has reported about 94 events as seen in Figure 11 . The spread of the events is diffuse and randomly distributed over the specimen volume (microcracking at points of stress singularity in concrete). From points 1 to 4 during the drop in load, microcracking becomes more localized around the notch and coalescing into major crack that grows until the reinforcing bar. The number of AE events keep increasing in a narrow localized region above the notch in the mid-span region of the beam as seen in Figure 11. In this period, between points 1 and 4, as seen in Figure 12, the rate of increase in AE events is quite high as indicated by the large slope of the AE event curve. Beyond the point 4, the load gets transferred to the reinforcing bar and the load carrying capacity increases. The slope of the AE events drops with increase in the number of events until point 10 as seen in Figure 14. At this point (point 10), the yielding begins in the rebar with increasing displacements while the load remains almost constant upto point 12. Even before the yielding begins in the rebar, the localized microcracking has reached the whole depth of beam with rebar carrying the major portion of the load. As yielding of the rebar occurs between points 10 and 12, the width of the band of events increases indicating an increase in crack width and CMOD.

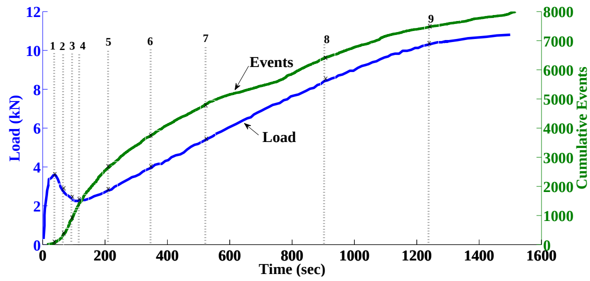

Figure 12: Plot of cumulative events and load versus time for a typical medium size specimen with 6mm bar (0.37%)

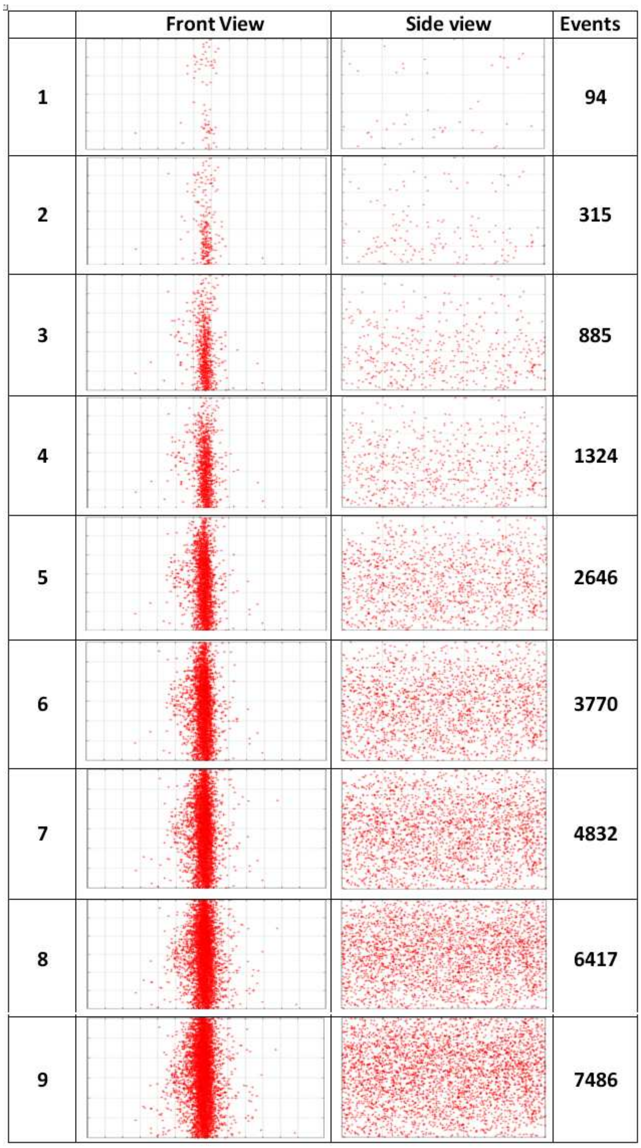

Figure 11: Location for AE events for specimen corresponding to points in the plot of cumulative events and load versus time for a typical medium size specimen with 6mm bar (0.37%)

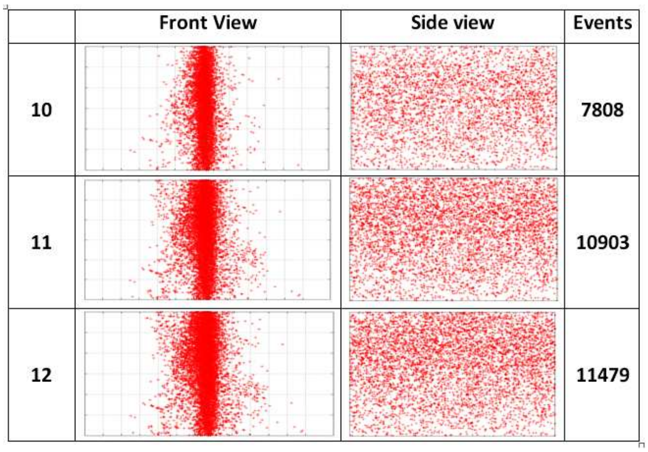

Figure 13: Location for AE events for specimen corresponding to points 10, 11 and 12 in the plot of cumulative events and load versus time for a typical medium size specimen with 6mm bar (0.37%)

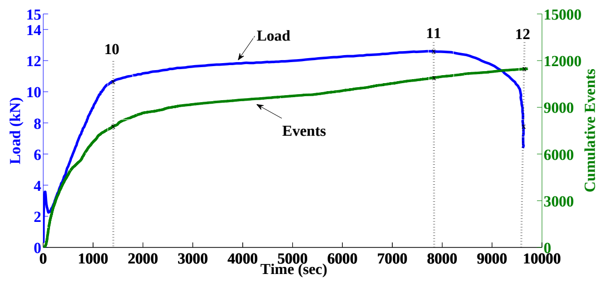

Figure 14: Plot of cumulative events and load versus time for a typical medium size specimen with 6mm bar (0.37%)

Figure 15 shows the cumulative absolute AE energy and load with time for the medium size specimen reinforced with 6mm diameter bar (0.37 %). Absolute energy is defined as the integral of the squared voltage signal divided by the reference resistance (10k-Ohm) over the duration of AE wave form. This is the true energy measure of AE hit. The unit of absolute energy is atto Joules. Absolute energy is selected from the maximum value of absolute energy from all the sensors [15, 16]. It is seen that there is a continuous increase in the cumulative absolute AE energy with time until failure of the specimen. The absolute AE energy follows the same pattern as the cumulative AE events.

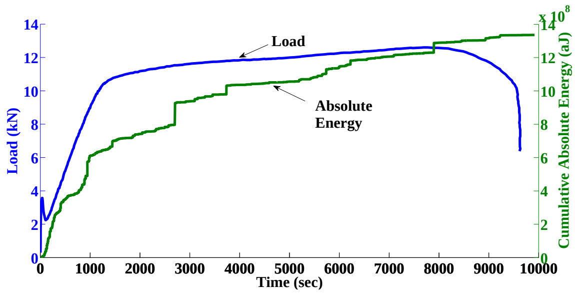

Figure 15: Plot of cumulative absolute energy and load versus time for a typical medium size specimen with 6mm bar (0.37%)

Figures 16 and 17 shows the results of cumulative AE events versus time and cumulative absolute energy versus time respectively for all sizes and reinforcement ratios of beams. Figure 18 shows the load versus time for comparison with these specimens. It is seen that the cracking behavior in all the under-reinforced concrete beams are very similar as reflected in the AE events and AE energy plots. The AE events and AE energy are continuously increasing until yielding in the reinforcing bar begins and remains constant thereafter upto failure. Comparing the results of the two large beams having different reinforcement ratios, it is seen that the beam with higher reinforcement ratio has larger number of AE events being formed until failure. This implies that higher reinforcement ratio in under-reinforced beams has a tendency to increase the number of microcracks occurring in concrete. However, the cumulative AE energy remains almost the same for these two large specimens having different reinforcement ratios.

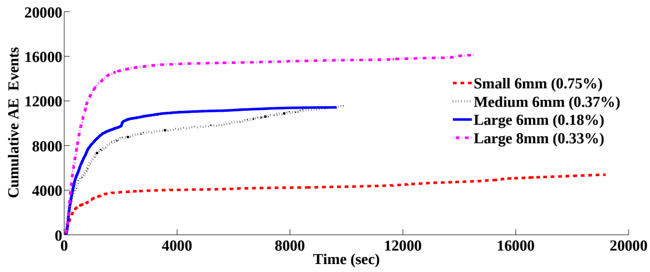

Figure 16: Plot of cumulative events versus time for small 6mm (0.75%), medium 6mm (0.37%), large 6mm (0.18%) and large 8mm (0.33%)

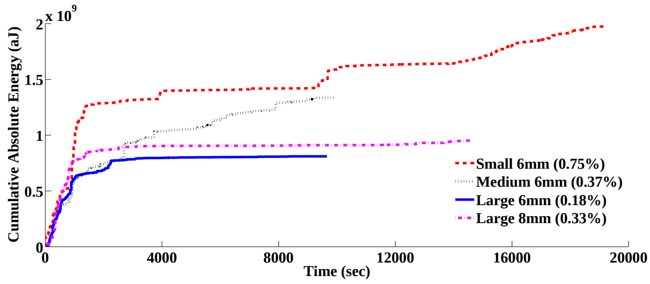

Figure 17: Plot of cumulative absolute AE energy versus time for small 6mm (0.75%), medium 6mm (0.37%), large 6mm (0.18%) and large 8mm (0.33%)

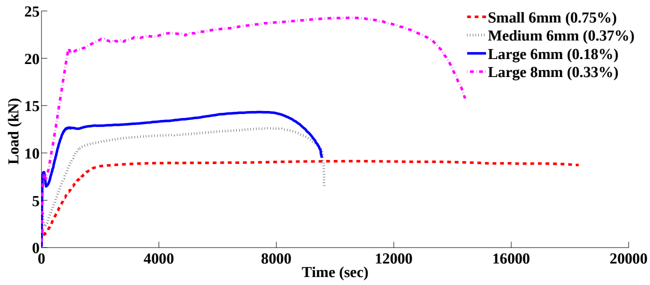

Figure 18: Plots of load versus time for small 6mm (0.75%), medium 6mm (0.37%) , large 6mm (0.18%) and large 8mm (0.33%)

Figures 19 20 21 22 shows the photograph of the failure pattern of small 6mm (0.75%), medium 6mm (0.37%), large 6mm (0.18%) and large 8mm (0.33%) respectively. It is seen that beam has failed under flexure with yielding in reinforcement followed by the propagation of single discrete crack at the mid-span which is a characteristic feature of under-reinforced concrete beams.

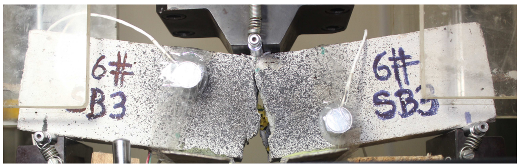

Figure 19: Failure pattern for small 6mm (0.75%)

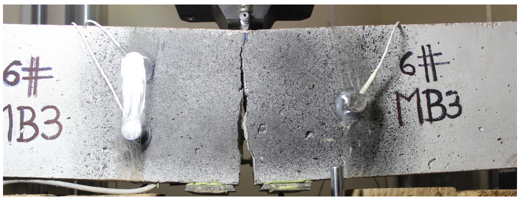

Figure 20: Failure pattern for medium 6mm (0.37%),

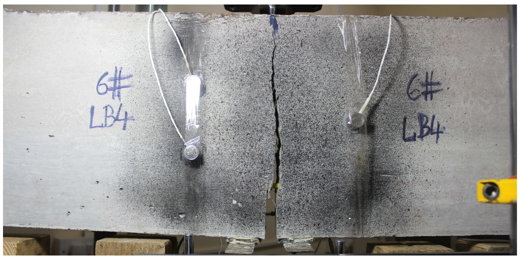

Figure 21: Failure pattern for large 6mm (0.18%)

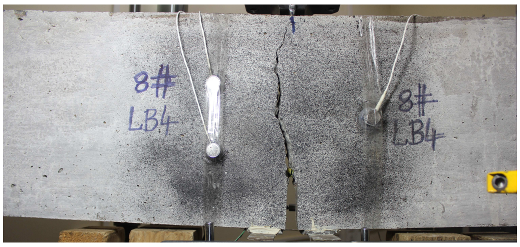

Figure 22: Failure pattern for large 8mm (0.33%

5 Conclusions

AE technique is used to study the fracture behavior in under-reinforced concrete beam specimens. The specimens were reinforced with single longitudinal bar and no shear reinforcement were provided. In this study, under-reinforced concrete beam of small 6mm (0.75%), medium 6mm (0.37%), large 6mm (0.18%) and large 8mm (0.33%) were considered. The specimens were tested in three point bending under CMOD control in the closed loop servo controlled hydraulic testing machine to understand their behavior using acoustic emission technique.

From this paper, the following conclusions are made:

- The plots of load versus CMOD and load versus midspan displacement for all under-reinforced concrete beams shows that the slopes of initial segment are overlapping with each other. This is due to the fact that only the stiffness of plain concrete is reflected and the reinforcement has not yet come into action. The first peak in the load corresponds to the load transfer mechanism to the steel bar and substantial increase of longitudinal strain. The maximum load is reached in the respective beams when the strain in the rebar has reached its yield value which is in the range of 3500 to 3800 microstrains. As the plastic strains increase in the reinforcement the CMOD and mid-span displacement increases substantially at constant load indicating a ductile behavior which is the main characteristic of under-reinforced concrete beams.

- The spread of the acoustic emission events and its distribution within the beams help in understanding the fracture processes. They provide information regarding the sequence of mechanisms taking place such as micro-cracking, coalescing of microcracks to macrocracks, increased width of macro-cracking and final fracture in under-reinforced concrete beams.

- The results of AE such as events, absolute energy are useful in understanding in cracking and fracture processes for different sizes of beam having different reinforcement ratio. The AE events and absolute energy are continuously increasing until yielding in the reinforcing bar begins and remains constant thereafter until failure occurs.

REFERENCES

[1] G Ruiz, M Elices, and J Planas. Experimental study of fracture of lightly reinforced concrete beams. *Materials and Structures*, 31(10):683–691, 1998.

[2] Dragoslav Sumarac, Miodrag Sekulovic, and Dusan Krajcinovic. Fracture of reinforced concrete beams subjected to three point bending. *International Journal of Damage Mechanics*, 12(1):31–44, 2003.

[3] Alessandro P Fantilli, Daniele Ferretti, and Gianpaolo Rosati. Effect of bar diameter on the behavior of lightly reinforced concrete beams. *Journal of Materials in Civil Engineering*, 17(1):10–18, 2005.

[4] Gonzalo Ruiz and Jacinto R Carmona. Experimental study on the influence of the shape of the cross-section and the rebar arrangement on the fracture of LRC beams. *Materials and Structures*, 39(3):343–352, 2006.

[5] Shohei Momoki, Hwakian Chai, Dimitrios G Aggelis, Akinobu Hirama, and Tomoki Shiotani. Acoustic emission for characterizing behavior of composite concrete elements under flexure. *Journal of Acoustic Emission*, 27:186–193, 2009.

[6] Manindra R Kaphle, Andy CC Tan, David P Thambiratnam, and Tommy HT Chan. Study of acoustic emission data analysis tools for structural health monitoring applications. In *Progress in Acoustic Emission XV: Proceedings of the 20th International Acoustic Emission Symposium*. Japanese Society for Non-Destructive Inspection, 2010.

[7] Alberto Carpinteri, Giuseppe Lacidogna, and Gianni Niccolini. Damage analysis of reinforced concrete buildings by the acoustic emission technique. *Structural Control and Health Monitoring*, 18(6):660–673, 2011.

[8] R Vidya Sagar and MVMS Rao. An experimental study on loading rate effect on acoustic emission based b-values related to reinforced concrete fracture. *Construction and Building Materials*, 70:460–472, 2014.

[9] R Vidya Sagar. Acoustic emission characteristics of reinforced concrete beams with varying percentage of tension steel reinforcement under flexural loading. *Case Studies in Construction Materials*, 6:162–176, 2017.

[10] Domenico Luca Carnì, Carmelo Scuro, Francesco Lamonaca, Renato Sante Olivito, and Domenico Grimaldi. Damage analysis of concrete structures by means of acoustic emissions technique. *Composites Part B: Engineering*, 115:79–86, 2017.

[11] Giuseppe Lacidogna, Gianfranco Piana, and Alberto Carpinteri. Damage monitoring of three-point bending concrete specimens by acoustic emission and resonant frequency analysis. *Engineering Fracture Mechanics*, 210:203–211, 2019.

[12] MH Prashanth, Parvinder Singh, and JM Chandra Kishen. Role of longitudinal reinforcement on the behavior of under reinforced concrete beams subjected to fatigue loading. *International Journal of Fatigue*, 125:271–290, 2019.

[13] MH Prashanth. *Experimental investigations into fracture and fatigue behavior of plain and reinforced concrete beams using acoustic emission technique*. PhD thesis, Indian Institute of Science, Bangalore, 2018.

[14] Eric N Landis. Micro–macro fracture relationships and acoustic emissions in concrete. *Construction and Building Materials*, 13(1):65–72, 1999.

[15] S Muralidhara, BK Raghu Prasad, Hamid Eskandari, and Bhushan Lal Karihaloo. Fracture process zone size and true fracture energy of concrete using acoustic emission. *Construction and Building Materials*, 24(4):479–486, 2010.

[16] K Otsuka, H Date, and T Kurita. Fracture process zone in concrete tension specimens by X-ray and AE techniques. In *Proceedings of Fracture Mechanics of Concrete Structures, FraMCoS-3*, pages 3–16, 1998.